Astron. Astrophys. 354, 874–880 (2000)

ASTRONOMY AND ASTROPHYSICS

The oxygen abundance deficiency in irregular galaxies

L.S. Pilyugin[1] **and F. Ferrini**[2,⋆]

[1] Main Astronomical Observatory of National Academy of Sciences of Ukraine, Goloseevo, 03680 Kiev-127, Ukraine (pilyugin@mao.kiev.ua)
[2] Department of Physics, Section of Astronomy, University of Pisa, Piazza Torricelli 2, 56100 Pisa, Italy (federico@astr2pi.difi.unipi.it)

Received 29 October 1999 / Accepted 13 December 1999

Abstract. The observed oxygen abundances in a number of irregular galaxies have been compared with predictions of the closed-box model of chemical and photometric evolution of galaxies. Oxygen is found to be deficient with respect to the predicted abundances. This is an indicator in favor of loss of heavy elements via galactic winds or/and of infall of low–abundance gas onto the galaxy.

The oxygen abundance deficiency observed within the optical edge of a galaxy cannot be explained by mixing with the gas envelope observed outside the optical limit. We confirm the widespread idea that a significant part of the heavy elements is ejected by irregular galaxies in the intergalactic medium.

Key words: galaxies: abundances – galaxies: evolution – galaxies: ISM – galaxies: irregular

1. Introduction

Irregular galaxies gained a central position in extragalactic studies, as the most abundant and least evolved galaxies in the universe. It was soon understood that they are not closed systems, and that galactic winds had to play a relevant role in their chemical evolution.

The hydrodynamic simulations of irregular galaxies lead to conflicting conclusions: de Young & Gallagher (1990), de Young & Heckman (1994) and MacLow & Ferrara (1999) found that irregulars can lose a significant fraction of metals via galactic winds; conversely, Silich & Tenorio-Tagle (1998) concluded that a low-density gaseous halo can inhibit the loss of matter from dwarf galaxies. Models of chemical evolution of irregular galaxies suggested that galactic winds can explain the chemical properties of these objects (Matteucci & Chiosi 1983; Matteucci & Tosi 1985; Pilyugin 1993, 1996; Marconi et al. 1994; Bradamante et al. 1998, and many others). Outflows of ionized gas have been observed in a number of irregular galaxies (Marlowe et al. 1995). Skillman (1997) has summarized the pros and cons for galactic wind–dominated evolution of irregular galaxies and has concluded that neither case is very strong.

Send offprint requests to: L.S. Pilyugin
⋆ *Present address:* INTAS, 58 Avenue des Arts, 1000 Bruxelles, Belgium

In our previous work (Pilyugin & Ferrini 1998), we defined the oxygen abundance deficiency in galaxies as 1 minus the ratio of the observed oxygen abundance to that predicted by the closed-box model for the same gas mass fraction. Variations of the oxygen abundance deficiency from galaxy to galaxy can only be caused by differences in gas exchange between galaxies and their environments. In turn, the oxygen abundance deficiency can be considered as an indicator of mass exchange, in particular by galactic winds. The goal of the present study is to study this problem quantitatively. In Sect. 2 we present the observational data base. The stellar mass to luminosity ratio in irregular galaxies is derived in Sect. 3, the values of the oxygen abundance deficiency for a number of irregulars are obtained in Sect. 4. Sect. 5 contains discussion and a summary.

2. Observational data

The data base used in this study consists of published B magnitudes of irregular galaxies, B–V colors, distances, oxygen abundances, HI emission fluxes, and radial distributions of HI. The variations in oxygen abundance from region to region in the best studied irregular galaxies are always within the observational errors (Pagel et al. 1978; Skillman et al. 1989a) and there is no detectable radial oxygen abundance gradient. Then, the chemical composition of irregular galaxy can be specified by a single parameter.

Our sample contains 25 irregular galaxies for which we have collected the relevant observational data, given with references in Table 1. The commonly used name(s) are given in Columns 1 and 2, the Hubble type (T from de Vaucouleurs et al. 1991, RC3) in Column 3, the adopted distance in Column 4 (references in Column 5). The cepheid distances are labeled with letter c. The B luminosity computed from the adopted distance and the B_0^T magnitude from RC3 is given in Column 6, and the mass of atomic hydrogen from the m_{21} magnitude from RC3 in Column 7. The B-V color from RC3 is given in Column 8 and the oxygen abundance in Column 9 (references in Column 10).

3. Stellar mass to luminosity ratio

Irregular galaxies can contain a large amount of dark matter (Carignan & Beaulieu 1989; Kumai & Tosa 1992) which might

Table 1. Observational characteristics (with references) for the galaxies included in the present sample

name	other name	T type	distance Mpc	ref	logL_B	logM_{HI}	B-V	12+log O/H	ref
WLM	DDO 221	10	0.95 c	MF,LFM,SC	7.92	7.80	0.31	7.74	STM
NGC55		9	1.45	G	9.47	8.99	0.38	8.34	RM
IC10		10	0.83 c	SHKD,WWRSH	8.76	7.96	1.08:	8.18	LPRSTP
SMC		9	0.06 c	F	8.82	8.68	0.36	8.03	RM
IC1613	DDO 8	10	0.75 c	MF,LFM	8.02	7.80	0.65	7.71	RM
NGC1156		10	7.80	KMG	9.44	9.03	0.38	8.23	VSC
NGC1569	7 Zw 16	10	2.01	KT	9.02	7.97	0.23	8.16	RM
LMC		9	0.05	LFM	9.31	8.58	0.43	8.35	RM
NGC2366	DDO 42	10	3.44 c	TSHM	8.85	8.91	0.45	7.92	RM
DDO47		10	4.27	GKT	8.05	8.44	0.45	7.85	SKH
HolmbergII	DDO 50	10	3.05 c	HSD	8.80	8.82	0.39	7.92	RM
DDO53		9	3.40	KT	7.49	7.81	0.31	7.62	SKH
Leo A	DDO 69	10	2.20 c	HSKD	7.80	7.87	0.26	7.30	SKH
Sex B	DDO 70	10	1.44 c	MF	7.88	7.65	0.47	8.11	MAM
NGC3109	DDO 236	9	1.36 c	MPC	8.66	8.74		8.06	RM
Sex A	DDO 75	10	1.45 c	SMF	7.82	7.94	0.35	7.49	SKH
IC2574	DDO 81	9	3.40	KT	9.12	9.05	0.34	8.08	RM
NGC4214		10	4.10	Letal	9.37	9.05	0.43	8.23	RM
NGC4449		10	5.40	HT	9.69	9.47	0.37	8.32	SKH
GR8	DDO 155	10	2.24 c	TSHD	7.04	7.00	0.30	7.68	MAM
NGC5253		10	4.09 c	Setal	9.23	8.36	0.28	8.16	PSTE, RSRWR
NGC5408	Tol 116	10	3.24	RM	8.54	8.21	0.42	8.01	RM
IC4662		10	2.00	H-MMM	8.29	8.08	0.29	8.06	H-MMM
NGC6822		10	0.51 c	MF,LFM	8.25	7.84		8.23	RM
Pegasus		10	0.76	Getal	6.77	6.51	0.54	7.93	SBK

Note to table:
The cepheid distances are labeled with letter c.
The B-V value for IC10 is taken from VSC.
HI measurement for DDO53 is taken from vDetal

List of references to table: F – Freedman (1988); G – Graham (1982); Getal – Gallagher et al. (1998); GKT – Georgiev et al. (1997); H-MMM – Heydari-Malayeri et al. (1990); HSD – Hoessel et al. (1998); HSKD – Hoessel et al. (1994); HP – Hunter & Plummer (1996); KMG – Karachentsev et al. (1996); KSRWR – Kobulnicky et al. (1997); KT – Karachentsev & Tikhonov (1994); Letal – Leitherer et al. (1996); LFM – Lee et al. (1993); LPRSTP –Lequeux et al. (1979); MAM – Moles et al. (1990); MF – Madore & Freedman (1991); MPC – Musella et al. (1997); PSTE – Pagel et al. (1992); RM – Richer & McCall (1995); SC – Sandage & Carlson (1985); SBK – Skillman et al. (1997); Setal – Sandage et al. (1994); SHKD – Saha et al. (1996); SKH – Skillman et al. (1989a); SMF – Sakai et al. (1996); STM – Skillman et al. (1989b); TSHD – Tolstoy et al. (1995a); TSHM – Tolstoy et al. (1995b); vDetal – van Driel et al. (1998); VSC – Vigroux et al. (1987); WWRSH – Wilson et al. (1996)

not take part directly to the chemical evolution. The luminous mass (mass of gas, stars, and stellar remnants) should be used rather than the dynamical mass in investigations of the chemical properties of irregular galaxies. The mass of stars M_s including stellar remnants can be derived from the luminosity of the galaxy if the stellar mass to light ratio $\Upsilon_s = M_s/L_B$ can be determined. It depends on the star formation history (SFH) in the galaxy. For a few nearby irregular galaxies the star formation history can be derived from the color-magnitude diagram of a large number of individual stars. Such determinations exist for the LMC (Butcher 1977; Frogel 1984; Bertelli et al. 1992; Elson et al. 1994), NGC 6822 (Gallart et al. 1996a, b), the Pegasus dwarf (Aparicio et al. 1997; Gallagher et al. 1998), and Sextans A (Dohm-Palmer et al. 1997). Two variants of star formation histories will be used for Pegasus dwarf according to two different estimates of the distance: 0.95 Mpc from Aparicio et al. (1997), and 0.76 Mpc from Gallagher et al. (1998).

Using our model for the chemical and photometric evolution of an one-zone system (Pilyugin & Ferrini 1998), the mass to luminosity ratios M_s/L_B and colors U-B and B-V have been computed for galaxies with known star formation histories. The case S of nucleosynthesis has been adopted (Pilyugin & Ferrini 1998). The computed and observed U-B and B-V colors as well as the computed star mass to luminosity ratios of these galaxies are given in Table 2. The observed colors of galaxies were taken from RC3 if not indicated otherwise.

The computed positions of galaxies from Table 2 in the M_s/L_B - (B-V) diagram are shown in Fig. 1.

The Hubble sequence has been related to star formation histories (see e.g. Sandage 1986); in particular it is expected that the average star formation rate in irregular galaxy increases slightly

Table 2. Observed $(U-B)_O$, $(B-V)_O$, computed $(U-B)_C$, $(B-V)_C$ colors, and computed stellar mass to luminosity ratio M_s/L_B for irregular galaxies with known star formation histories. The observed colors are taken from RC3 for the LMC and the Pegasus dwarf, and from Hunter & Plummer (1996) for Sextans A.

Galaxy	$(U-B)_O$	$(U-B)_C$	$(B-V)_O$	$(B-V)_C$	M_s/L_B
LMC	– 0.06	– 0.08	0.43	0.44	0.47
NGC6822		– 0.37		0.24	0.35
Pegasus[1]	0.06	– 0.07	0.54	0.48	0.75
Pegasus[2]	0.06	0.02	0.54	0.59	0.94
Sextans A	– 0.36	– 0.38	0.26	0.24	0.29

Notes to table:
1 – SFH from Aparicio et al. (1997);
2 – SFH from Gallagher et al. (1998)

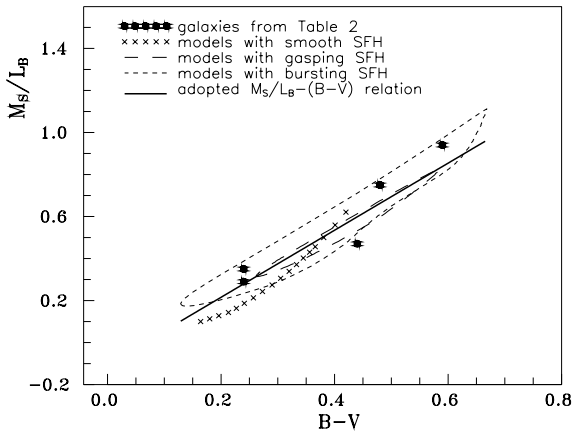

Fig. 1. The positions of galaxies with known star formation history (SFH) (filled circles) in the diagram stellar mass to luminosity ratio M_s/L_B versus B-V. These positions are compared with the results of models with smooth SFHs (crosses) for different values of τ, and of models with gasping (long-dashed line) and bursting (short-dashed line) SFHs for different values of t_0. The solid line is the M_s/L_B – (B-V) relationship adopted in this paper.

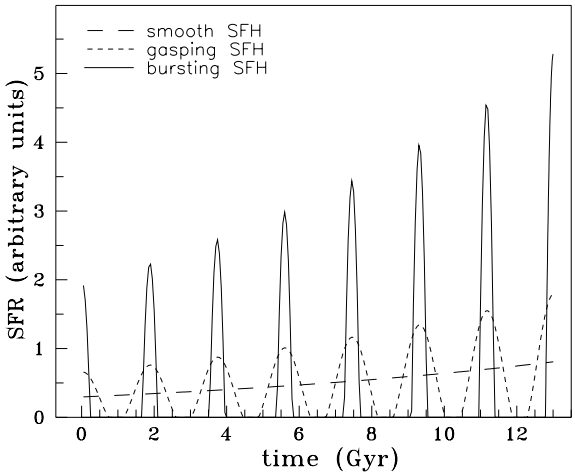

Fig. 2. Continuous (long-dashed line), bursting (solid line), and gasping (short-dashed line) star formation histories (SFH).

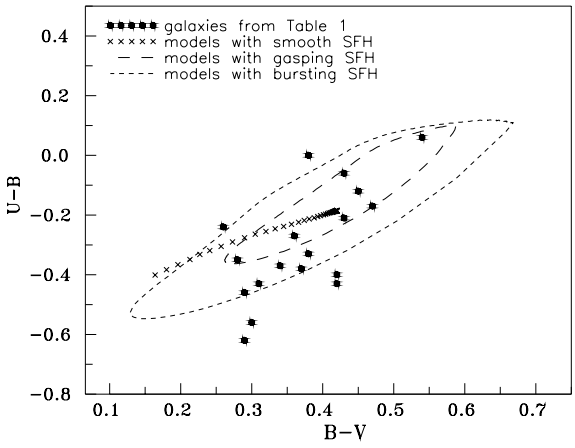

Fig. 3. The positions of galaxies (filled circles) in the U-B, B-V two color diagram. They are compared with the results of models with continuous SFHs (crosses) for different values of τ, models with gasping (long-dashed line) and bursting (short-dashed line) SFHs for different values of t_0.

with time. Since we are not interested here in the comprehension of the physics of the evolution of irregulars, we adopt simple analytical expressions for the star formation rate, depending on a time scale τ:

$$\psi(t) \propto \exp(t/\tau). \quad (1)$$

A grid of models with smooth star formation history for different values of τ from 1 Gyr (a strongly increasing star formation rate) to 500 Gyr (an almost constant star formation rate) have been computed. The star formation history with τ=13 Gyr is shown in the Fig. 2 by a long-dashed line. The positions of these models in the M_s/L_B versus B-V diagram are shown in the Fig. 1 by crosses. The agreement between these models and the representative points of galaxies is not good. In particular, the values of B-V larger than ~ 0.4 observed in some irregulars cannot be reproduced. The predictions of these models together with positions of galaxies from Table 1 are shown in Fig. 3 in the U-B, B-V diagram. It is clear that models with smooth star formation histories cannot reproduce the observed positions of irregular galaxies in this diagram.

This disagreement is a consequence of the hypothesis that the SFH is smooth. Actually star formation in irregular galaxies is not snooth: active periods alternate with quiet periods. In order to take this into account, models with non–smooth star formation histories have been computed. We describe it by the expression

$$\psi(t) \propto \begin{cases} A(t)\ \exp(t/\tau) & \text{if} \quad A(t) > 0, \\ 0 & \text{if} \quad A(t) \leq 0, \end{cases} \quad (2)$$

where

$$A(t) = cos(t/\tau_P + t_0) + c. \quad (3)$$

The parameter τ_P, which indicates the number of cycles of star formation during the lifetime of a galaxy t_{gal} (that we adopted to be t_{gal} = 13Gyr), is defined as

$$t_{gal}/\tau_P = 2n\pi. \quad (4)$$

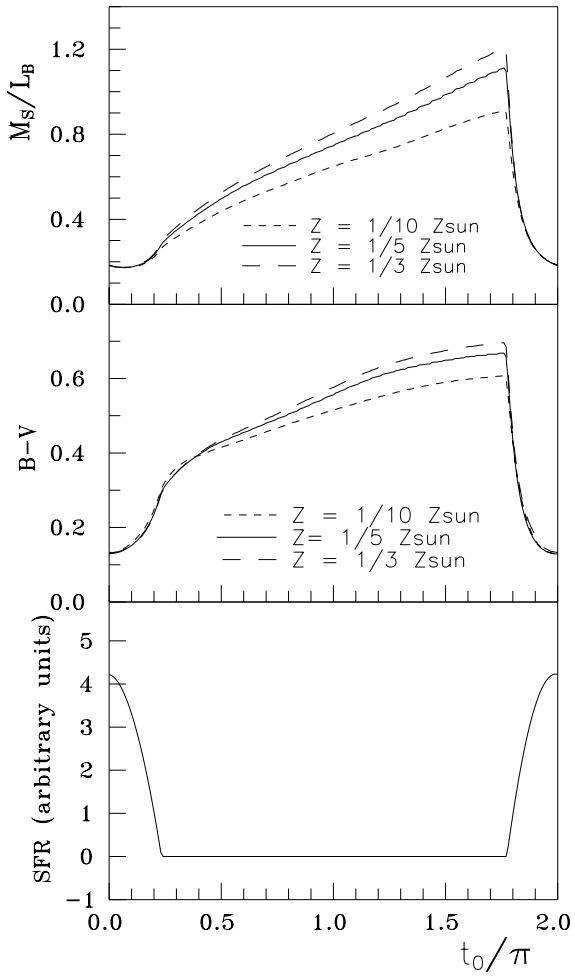

Fig. 4. The present–time star formation rate, the B-V color, and the M_s/L_B ratio as functions of t_0 for models with bursting star formation history.

Each cycle consists of an epoch with active star formation and an epoch without star formation. Their relative duration is governed by the parameter c. The case $c = 0$ corresponds to a periodic star formation history, in which the durations are equal. The values $-1 < c < 0$ corresponds to shorter epochs with active star formation. This case will be referred to as a "bursting" star formation history. The case with c = –0.75, τ = 13 Gyr, t_0 = 0, and n = 7 is shown in Fig. 2. The values $0 < c < 1$ corresponds to the opposite case. Following Tosi (1993), this case will be referred to as a "gasping" star formation history. The case with c = 0.75, τ = 13 Gyr, t_0 = 0, and n = 7 is shown in Fig. 2. The point in the cycle of star formation at the present time is governed by the choice of t_0 (Fig. 4). As it can be seen in Fig. 4, the B-V color and stellar mass to luminosity ratio M_s/L_B are strongly dependent on t_0 (Fig. 4 shows the evolutionary change of B-V and M_s/L_B during the last cycle of star formation). The values of B-V and M_s/L_B have a maximum at the point just before the beginning of the star formation phase. The values B-V and M_s/L_B decrease with increasing of star formation rate, pass through a minimum at the maximum star formation rate, and then increase.

A grid of models with gasping star formation history has been computed. The positions of these models in the M_s/L_B versus (B-V) diagram for various values of t_0 and for fixed values of other parameters (τ=13 Gyr, n=7, c=0.75) are shown in Fig. 1. A similar grid of models with bursting star formation history has also be computed with τ=13 Gyr, n=7, c=–0.75 (Fig. 1). The fit with observations is now good. It is also good in the U-B versus B-V diagram. Some remaining discrepancies might be explained by the contribution of the ionized gas emission to the radiation of galaxy, which is not taken into account in the present models. Figs. 1 and 3 suggest that the mass to luminosity ratio for and irregular galaxy with unknown star formation history can be estimated from its measured B-V color and relationship between stellar mass to luminosity ratio and B-V color.

Up to here we have only considered models with a fixed present oxygen abundance 12+log O/H=8.2 ($O/H \approx 1/5(O/H)_\odot$). The mass to luminosity ratio depends not only on the star formation history but also on the metallicity. To examine the dependence of the mass to luminosity ratio on the metallicity, models with bursting star formation history and with present oxygen abundances 12+log O/H=7.9 ($O/H \approx 1/10(O/H)_\odot$) and 12+log O/H=8.4 ($O/H \approx 1/3(O/H)_\odot$) have been computed. For the range of observed B-V (0.3 to 0.5) the differences in M_s/L_B predicted by models with 12+log O/H=7.9 and 12+log O/H=8.4 with those predicted by models with 12+log O/H=8.2 are smaller than 15 per cent (Fig. 4). On the other hand, Fig. 5 shows that there is no correlation between B-V and the present-day oxygen abundance. This shows that B-V is mainly determined by the star formation history in the recent past. Therefore the relationship between stellar mass to luminosity ratio M_s/L_B and B-V color can be considered as independent on the present oxygen abundance.

We adopt as a first approximation a linear relationship between mass to luminosity ratio M_s/L_B and B-V color (Fig. 1)

$$\Upsilon_s = -0.10 \pm 0.15 + 1.60\,(B-V). \quad (5)$$

The error on the intercept includes the range of models.

4. Oxygen abundance deficiency in irregular galaxies

4.1. Hydrogen content in irregular galaxies

The size of irregular galaxies in HI is larger than their optical size (Salpeter & Hoffman 1996, and references therein). As we have seen, the variations of oxygen abundance from region to region in the best studied irregular galaxies are within observational errors, a strong evidence that irregular galaxies are well mixed system inside the optical diameter. If the zone of the mixing extends to the outer HI then the gas outside the optical diameter can contain a significant part of the heavy elements produced by the stars and, therefore, can play an important role in the chemical evolution of the galaxy. Hunter & Gallagher (1985) have found that the presence or absence of extended HI envelopes does not appear to be reflected in the properties of the

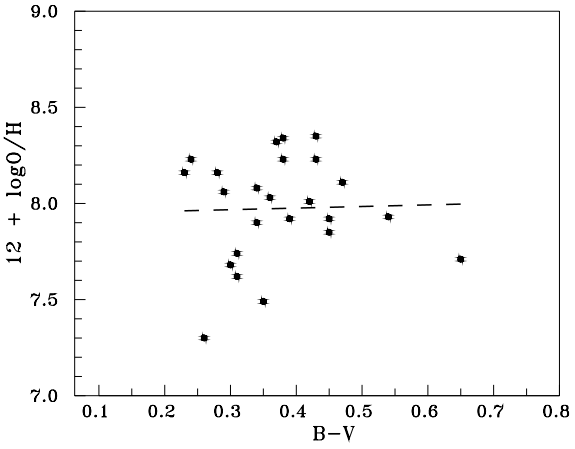

Fig. 5. The positions of irregular galaxies from our sample in the B-V versus O/H diagram. The line is the formal best fit to the data. There is no correlation between the B-V color and the present-day oxygen abundance.

optical components of irregular galaxies. They concluded that only the gas within the optical limit plays an important role in the life of a galaxy.

The mass of atomic hydrogen in the irregular galaxies listed in Table 1 is the total mass. For a number of irregular galaxies from our sample there are measurements of radial distribution of surface mass density of atomic hydrogen that allows to determine the fraction of HI mass within the optical diameter f_{opt}. Table 3 gives the fraction f_{opt} and the ratio of the hydrogen radius R_H (radius at face-on surface mass density of atomic hydrogen of 1 $M_\odot\, pc^{-2}$) to the optical radius R_{25} (from RC3). Table 3 shows the fraction of HI mass within the optical diameter of a galaxy varies widely from f_{opt} = 0.36 for GR 8 to f_{opt} = 0.92 for NGC 55.

4.2. Oxygen abundance deficiency in irregular galaxies

The gas mass fraction μ is defined as

$$\mu = M_g/(M_g + M_s), \tag{6}$$

where M_g is the mass of gas within the optical radius R_{25} of the galaxy. The mass of stars is derived from the blue luminosity and the mass to luminosity ratio Υ_s

$$M_s = \Upsilon_s \times L_B. \tag{7}$$

The values of Υ_s computed using relation (5) are listed in Column 2 of Table 4. The mass of gas within the optical edge of a galaxy is taken as

$$M_{gas} = f_{opt} \times (1.4 \times (1 + r_{H_2}) \times M_{HI}) \tag{8}$$

where the factors r_{H_2} and 1.4 are introduced to take the contributions of molecular hydrogen and helium to gas mass into account, respectively. f_{opt} comes from Table 3. The correction for the presence of molecular hydrogen is uncertain since the H_2 content has been determined from CO line observations in a few irregular galaxies only. Fortunately, the average global H_2 to HI mass ratio $r_{H_2} = H_2/HI$ is not large for these galaxies, r_{H_2} = 0.2±0.04, (Israel 1997). Here we adopt r_{H_2} = 0.2 for all the galaxies. The values of μ are given in Column 3 of Table 4.

The global oxygen abundance deficiency is defined as $\eta = 1 - Z_O^{obs}/Z_O^{CB}$. The values of η are given in Column 4 of Table 4. The positions of irregular galaxies in the μ – O/H diagram

Table 3. Fraction of atomic hydrogen mass within the optical diameter f_{opt}, hydrogen to optical radius ratio R_H/R_0, with references, for a number of irregular galaxies in the present sample

galaxy name	f_{opt}	R_H/R_{25}	ref
NGC 55	0.92	1.14	PCW
IC 1613	0.68	1.41	LS
NGC 1156	0.84	1.46	BW
NGC 2366	0.67	1.65	WKA
Holmberg II	0.56	1.79	PWBR
Leo A	0.51	1.84	YL
NGC 3109	0.61	1.50	JC
Sextans A	0.48	1.77	STTW
IC 2574	0.64	1.40	MCR
GR 8	0.36	2.02	CBF

List of references to table: BW – Broeils & van Woerden (1994); CBF – Carignan et al. (1990); JC – Jobin & Carignan (1990); LS – Lake & Skillman (1989); MCR – Martimbeau et al. (1994); PCW – Puche et al. (1991); PWBR – Puche et al. (1992); STTW – Skillman et al. (1988); WKA – Wevers et al. (1986); YL – Young & Lo (1996)

Table 4. Computed characteristics (star mass to luminosity ratio $\Upsilon_s = M_s/L_B$, gas mass fraction μ, oxygen abundance deficiency η, and total luminous mass to luminosity ratio $\Upsilon_t = M_t/L_B$) for the irregular galaxies of the present sample

		within R_{25}			within R_H		
name	Υ_s	μ	η	Υ_t	μ	η	Υ_t
WLM	0.40				0.76	0.71	1.67
NGC55	0.51	0.50	0.55	1.02	0.52	0.52	1.06
SMC	0.48				0.72	0.54	1.69
IC1613	0.94	0.42	0.92	1.63	0.52	0.89	1.95
NGC1156	0.51	0.52	0.64	1.06	0.56	0.58	1.16
NGC1569	0.27				0.36	0.80	0.42
LMC	0.47				0.40	0.66	0.78
NGC2366	0.62	0.68	0.70	1.91	0.76	0.57	2.55
DDO47	0.62				0.87	0.26	4.74
HolmbII	0.52	0.65	0.72	1.51	0.77	0.54	2.28
DDO53	0.40				0.90	0.43	3.91
Leo A	0.32	0.76	0.90	1.32	0.86	0.80	2.29
Sex B	0.65				0.60	0.64	1.64
Sex A	0.29	0.79	0.82	1.35	0.88	0.63	2.50
IC2574	0.44	0.67	0.57	1.36	0.76	0.36	1.87
NGC4214	0.59				0.58	0.56	1.39
NGC4449	0.49				0.67	0.25	1.50
GR8	0.38	0.59	0.87	0.93	0.80	0.69	1.91
NGC5253	0.35				0.39	0.78	0.57
NGC5408	0.57				0.58	0.74	1.36
IC4662	0.36				0.74	0.45	1.40
NGC6822	0.35				0.65	0.44	1.00
Pegasus	0.84				0.52	0.81	1.76

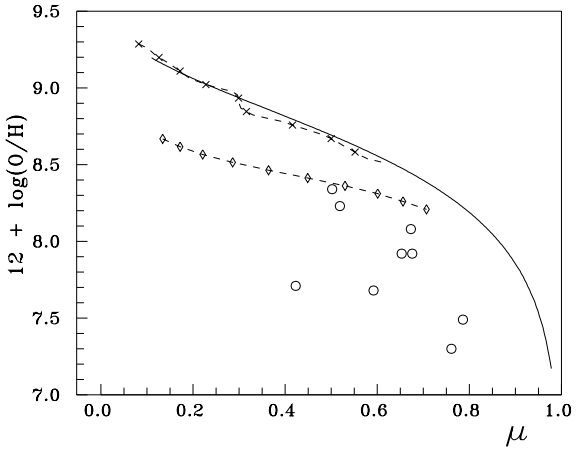

Fig. 6. The positions of irregular galaxies (open circles) in a diagram O/H vs. the gas fraction within the optical radius. The results of one-zone closed-box models with different present-day gas mass fraction (full curve) is presented by the solid line. The positions of two spiral galaxies NGC 5457 (crosses) and NGC 2403 (lozenges) are also shown for comparison. The data for these spirals are from Pilyugin & Ferrini (1998).

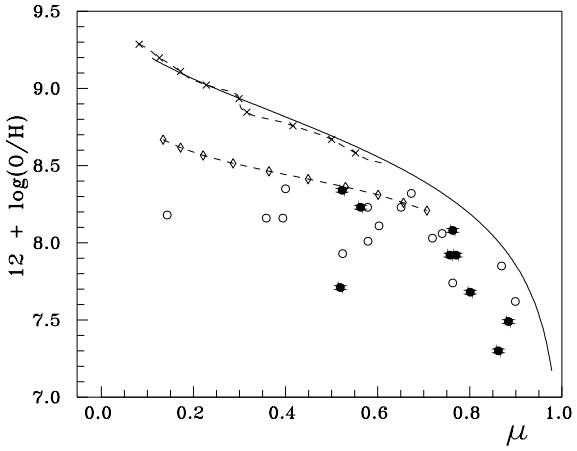

Fig. 7. Same as Fig. 6, but all the gas of the galaxy is now taken into consideration. The positions of irregular galaxies with known fraction of gas mass within the optical boundaries f_{opt} are shown by filled circles, and the positions of irregular galaxies with unknown f_{opt} are shown by open circles. The results of one-zone closed-box models with different present-day gas mass fraction (full curve) is presented by the solid line. The positions of two spiral galaxies NGC 5457 (crosses) and NGC 2403 (lozenges) are also shown for comparison. The data for these spirals are taken from Pilyugin & Ferrini (1998).

shown on Fig. 6 by circles. The curve defined by the one-zone closed-box models with different gas mass fraction (this curve will be referred to as standard curve) is shown in Fig. 6 as a solid line. For comparison we show the positions for various regions of the two spiral galaxies NGC 5457 (dashed line with crosses) and NGC 2403 (dashed line with lozenges) (data from Pilyugin & Ferrini 1998). NGC 5457 has no oxygen abundance deficiency, and NGC 2403 has the largest global oxygen abundance deficiency ($\eta = 0.57$) among the spiral galaxies considered by Pilyugin & Ferrini (1998). As it can be seen in Fig. 6, all the irregular galaxies are significantly displaced from the standard curve. Their values of oxygen abundance deficiency are also in excess of that in the dwarf spiral galaxy NGC 2403. The values of oxygen abundance deficiency range from ~ 0.5 to ~ 0.9. The relationships between the value of oxygen abundance deficiency and global parameters will be given in one of the next papers of this series.

Since irregular galaxies are gas-rich systems (as it can be seen from Table 4 the mass of gas component exceeds the mass of the stellar component in the galaxy) the total luminous mass to luminosity ratio $\Upsilon_t = M_t/L_B = (M_s + M_{gas})/L_B$ is significantly larger than the value of star mass to luminosity ratio Υ_s (compare the data from Columns 2 and 5 of Table 4).

Can the oxygen abundance deficiency within optical edge of irregular galaxy be explained by the mixing of interstellar matter with gas outside the optical edge? To study this possibility, the oxygen abundance deficiency have been re–computed under the assumption that all the gas associated with a galaxy is well mixed. In this case the mass of gas in the galaxy is

$$M_{gas} = 1.4 \times (1 + r_{H_2}) \times M_{HI}. \quad (9)$$

All the other values are derived in the same way as in the previous case. The values of μ, η, and M_t/L_B are listed in Columns 6-8 of Table 4.

The positions of irregular galaxies in the μ – O/H diagram in the present case are shown on Fig. 7: significant displacements of irregular galaxies relative to the standard curve remain. The inclusion of extended HI envelope outside the optical radius only slightly decreases the displacement of irregular galaxies relative to the standard curve.

5. Conclusions

We have found that all the irregular galaxies considered here have a significant oxygen abundance deficiency. This is a strong argument in favor of an important role of mass exchange with the environment in the chemical evolution of these galaxies. These conclusions remain even if one takes into consideration the gas envelope observed outside the optical edge. This confirm the widespread idea that a significant part of the heavy elements is ejected by irregular galaxies in the intergalactic medium.

We emphasize that the relation between oxygen abundance vs. gas mass fraction in the closed box model used in present study was constructed so that the positions of the most metal-rich giant spiral galaxies (including NGC 5457) in the μ -O/H diagram are fitted by this relation (Pilyugin & Ferrini 1998). Therefore the oxygen abundance deficiency of irregular galaxies can also be considered as relative to the giant spiral galaxy NGC 5457. It has been found by Pilyugin & Ferrini (1998) that the precise choice of the oxygen production by individual stars and of the parameters of the initial mass function are not critical in this differential comparison.

Acknowledgements. We thank Dr. N.Bergvall for his constructive comments on the manuscript. We thank the referee, Prof. J.Lequeux, for the suggestions and comments that improved sensibly the presentation. L.P. thanks the Staff of Department of Physics, Section of Astronomy

(University of Pisa) for hospitality. This study was partly supported by the INTAS grant No 97-0033.

References

Aparacio A., Gallart C., Bertelli G., 1997, AJ 114, 669
Bertelli G., Matteo M., Chiosi C., Bressan A., 1992, ApJ 388, 400
Bradamante F., Matteucci F., D'Ercole A., 1998, A&A 337, 338
Broeils A.H., van Woerden H., 1994, A&ASS 107, 129
Butcher J.A., 1977, ApJ 216, 372
Carignan C., 1985, ApJ 299, 59
Carignan C., Beaulieu S., 1989, ApJ 347, 760
Carignan C., Beaulieu S., Freeman K.C., 1990, AJ 99, 178
de Vaucouleurs G., de Vaucouleurs A., Corvin H.G., et al., 1991, Third Reference Catalog of bright Galaxies. Springer, New York, (RC3)
de Young D., Gallagher J., 1990, ApJ 356, L15
de Young D., Heckman T., 1994, ApJ 431, 598
Dohm-Palmer R.C., Skillman E.D., Saha A., et al., 1997, AJ 114, 2527
Elson R.A.W., Forbes D.A., Gilmore G.F., 1994, PASP 106, 632
Freedman W.L., 1988, ApJ 326, 691
Frogel J.A., 1984, PASP 96, 856
Gallagher J.S., Tolstoy E., Dohm-Palmer R.C., et al., 1998, AJ 115, 1869
Gallart C., Aparicio A., Bertelli G., Chiosi C., 1996a, AJ 112, 1950
Gallart C., Aparicio A., Bertelli G., Chiosi C., 1996b, AJ 112, 2596
Georgiev Ts.B., Karachentsev I.D., Tikhonov N.A., 1997, AZh Let. 23, 586
Graham J.A., 1982, ApJ 252, 474
Heydari–Malayeri M., Melnick J., Martin J.-M., 1990, A&A 234, 99
Hoessel J.G., Saha A., Danielson G.E., 1998, AJ 115, 573
Hoessel J.G., Saha A., Krist J., Danielson G.E., 1994, AJ 108, 645
Hunter D.A., Gallagher J.S., 1985, AJ 90, 1789
Hunter D.A., Plummer J.D., 1996, ApJ 462, 732
Israel F.P., 1997, A&A 328, 471
Jobin M., Carignan C., 1990, AJ 100, 648
Karachentsev I., Musella I., Grimaldi A., 1996, A&A 310, 722
Karachentsev I.D., Tikhonov N.A., 1994, A&A 286, 718
Kobulnicky H.A., Skillman E.D., Roy J.-R., Walsh J.R., Rosa M.R., 1997, ApJ 477, 679
Kumai Y., Tosa M., 1992, A&A 257, 511
Lake G., Skillman E.D., 1989, AJ 98, 1274
Lee M.G., Freedman W.L., Madore B.F., 1993, ApJ 417, 553
Leitherer C., Vacca W.D., Conti P.S., et al., 1996, ApJ 465, 717
Lequeux J., Peimbert M., Rayo J.F., Serrano A., Torres-Peimbert S., 1979, A&A 80, 155
MacLow M.-M., Ferrara A., 1999, ApJ 513, 142
Madore B.F., Freedman W.L., 1991, PASP 103, 933
Marconi G., Matteucci F., Tosi M., 1994, MNRAS 270, 35
Marlowe A.T., Heckman T.M., Wyse R.F.G., Schommer R., 1995, ApJ 438, 563
Martimbeau N., Carignan C., Roy J.-R., 1994, AJ 107, 543
Matteucci F., Chiosi C., 1983, A&A 123, 121
Matteucci F., Tosi M., 1985, MNRAS 217, 391
Moles M., Aparicio A., Masegosa J., 1990, A&A 228, 310
Musella I., Piotto G., Capaccioli M., 1997, AJ 114, 976
Pagel B.E.J., Edmunds M.G., Fosbury R.A.E., Webster B.L., 1978, MNRAS 184, 569
Pagel B.E.J., Simonson E.A., Terlevich R.J., Edmunds M.G., 1992, MNRAS 255, 325
Pilyugin L.S., 1993, A&A 277, 42
Pilyugin L.S., 1996, A&A 310, 751
Pilyugin L.S., Ferrini F., 1998, A&A 336, 103
Puche D., Carignan C., Wainscoat R.J., 1991, AJ 101, 447
Puche D., Westpfahl D., Brinks E., Roy J.-R., 1992, AJ 103, 1841
Richer M.G., McCall M.L., 1995, ApJ 445, 642
Saha A., Hoessel J.G., Krist J., Danielson G.E., 1996, AJ 111, 197
Sakai S., Madore B.F., Freedman W.L., 1996, ApJ 461, 713
Salpeter E.E., Hoffman G.L., 1996, ApJ 465, 595
Sandage A., 1986, A&A 161, 89
Sandage A., Carlson G., 1985, AJ 90, 1464
Sandage A., Saha A., Tammann G.A., et al., 1994, ApJ 423, L13
Silich S.A., Tenorio-Tagle G., 1998, MNRAS 299, 249
Skillman E.D., 1997, Rev. Mex. Astron. Astrofis. (Conf. Ser.) 6, 36
Skillman E.D., Bomans D.J., Kobulnicky H.A., 1997, ApJ 474, 205
Skillman E.D., Kennicutt R.C., Hodge P.W., 1989a, ApJ 347, 875
Skillman E.D., Terlevich R., Melnick J., 1989b, MNRAS 240, 563
Skillman E.D., Terlevich R., Teuben P.J., van Woerden H., 1988, A&A 198, 33
Tolstoy E., Saha A., Hoessel J.G., Danielson G.E., 1995a, AJ 109, 579
Tolstoy E., Saha A., Hoessel J.G., McQuade K., 1995b, AJ 110, 1640
Tosi M., 1993, In: Meylan G., Prugniel P. (eds.) Dwarf galaxies. ESO Proceedings No. 49, p. 465
Vigroux L., Stasinska G., Comte G., 1987, A&A 172, 15
van Driel W., Kraan-Korteweg R.C., Binggeli B., Huchtmeier W.K., 1998, A&AS 127, 397
Wevers B.M.H.R., van der Kruit P.C., Allen R.J., 1986, A&AS 66, 505
Wilson C.D., Welch D.L., Reid I.N., Saha A., Hoessel J., 1996, AJ 111, 1106
Young L.M., Lo K.Y., 1996, ApJ 462, 203